의학박사 학위논문

VEGFR-TKI 저항성을 가지는 전이성 투명세포 콩팥세포암종에서 mTOR 경로의 활성화를 통한 PD-L1 의 발현

PD-L1 expression
via Activation of mTOR Pathway in VEGFR-TKI Resistant
Metastatic Clear Cell Renal Cell Carcinoma

울 산 대 학 교 대 학 원

의 학 과

정 세 운

VEGFR-TKI 저항성을 가지는 전이성 투명세포 콩팥세포암종에서 mTOR 경로의 활성화를 통한 PD-L1 의 발현

지 도 교 수　　조 영 미

이 논문을 의학박사 학위 논문으로 제출함

2017 년　12 월

울 산 대 학 교 대 학 원

의　　학　　과

정　세　운

정세운의 의학박사학위 논문을 인준함

심사위원 이 재 련 인

심사위원 최 진 인

심사위원 김 경 은 인

심사위원 고 현 정 인

심사위원 조 영 미 인

울 산 대 학 교 대 학 원

2017 년 12 월

국문요약

Sunitinib 은 혈관 내피 세포 성장인자 경로를 목표로 하는 티로신 활성효소 억제제 중 하나로 전이성 투명세포 콩팥세포암종의 첫번째 치료제로 사용되고 있다. 하지만 대부분의 경우 재발하게 되며 환자는 결국 사망에 이르게 된다. 우리는 콩팥세포암종에서 티로신 활성효소 억제제가 PD-L1 과 관련하여 저항성을 가지게 되는 기전을 알아보고자 티로신 활성효소 억제제 치료 전과 후의 투명세포 콩팥세포암종 조직이 있는 10 개의 짝지어진 증례를 이용하여 치료 전, 후 유전자 발현의 차이와 연관되는 신호전달체계는 어떤 것이 있는지 알아보고, 또 다른 투명세포 콩팥세포암종 조직 109 증례를 면역조직화학 염색을 시행하여 입증하고 약물반응성 여부에 따라 두 그룹으로 나누어 무병생존분석을 시행하였다. 또한 sunitinib 에 감수성이 있는 신장암 세포주(769-P/suS)를 오랜 기간 sunitinib 에 노출시킴으로써 sunitinib 저항성 신장암세포주(769-P/suR)로 만들었고 이를 이용하여 세포 생존 실험, 정량역전사효소 중합효소연쇄반응, 웨스턴 블럿, 군집형성검사, 긁은자국검사, Matrigel 침입검사, 그리고 약물감수성 검사 등의 다양한 실험을 하였다. 그 결과, 10 례의 짝지어진 조직 검체 중 치료 후 조직에서 PD-L1 발현이 증가하였으며 이것은 mTOR 신호전달경로와 연관성이 있었다. 또한 109 증례의 투명세포 콩팥세포암종에서도 면역조직화학염색을 통해 PD-L1 의 발현이 mTOR 신호전달경로의 활성화와 유의한 관련이 있는 것으로 나타났으며, 약물반응성이 없는 그룹에서는 PD-L1 의 발현과 더 짧은 무병생존률과 의미 있는 관계가 있는 것으로 나타났다. 세포주 실험을 통하여 769-P/suR 에서 sunitinib 저항성이 있음을 확인하였고, 769-P/suS 에 비해 769-P/suR 에서 증식 능력, 이주 능력, 침입 능력이 훨씬 뛰어났으며, RNA 와 단백질 수준에서도 769-P/suR 에서 PD-L1, p-Akt, p-mTOR, pS6 의 발현량이 더 높게 나타났다. 769-P/suR 에 mTOR 억제제를 이용하여 mTOR 신호전달경로를 차단한 결과 PD-L1 의 발현량이 감소하였고 이주 능력, 침입 능력 또한 감소하는 것을 확인할 수 있었다. 이상의 결과를 종합하여 보았을 때 티로신 활성효소 억제제에 저항성이 있는 투명세포 콩팥세포암종 환자들의 일부에서는 mTOR 신호전달경로를 통하여 PD-L1 의 발현이 증가하며 이를 RNA, 단백질 수준 뿐 아니라 세포주 실험을 통하여 입증하였다.

차 례

표 목차

그림 목차

Introduction

Worldwide, the age-standardized rate (ASR) per 100,000 individuals for incidence of kidney cancer was 1.8 in less developed areas and it was 3.5 times higher in more developed areas in 2012. Similarly, the ASR for mortality of kidney cancer was 0.9 in less developed areas and it was 2 times higher in more developed areas.[1] Unfortunately, approximately one-third of patients eventually develop recurrences or distant metastases during follow up and require systemic treatment.[2,3] The prognosis of metastatic renal cell carcinoma (mRCC) is poor with 6–10 months of median survival and less than 20% of 2-year survival for untreated patients.[4,5]

Clear cell renal cell carcinoma (CCRCC) is the most common subtype of RCC, accounting for 65~70% of all RCC.[6] CCRCC is highly vascular tumor and it has a characteristic molecular alteration with inactivation of VHL gene and upregulation of hypoxia-inducible factors including vascular endothelial growth factor (VEGF).[7] Based on the carcinogenic mechanism, several tyrosine kinase inhibitors (TKI) targeting the vascular

endothelial growth factor receptor (VEGFR)-signaling pathway were developed and has been used as the first-line treatment. For example, sunitinib, one of the TKI inhibitor, demonstrated 42% of objective response rate, which exceeds those rates (5 to 20%) of conventional cytokine therapy.[8,9] Despite the initial response to TKI therapy, most mRCC patients eventually experience tumor recurrence due to resistance to the TKIs within 6–11 months of the treatment, requiring alternative therapeutic strategies for the TKI-resistant mRCC.[9-11] Furthermore, the underlying mechanism of the TKI-resistance needs to be fully defined.

Recently, immune checkpoint inhibitors, anti-programmed death (PD)-1 and PD-ligand 1 (L1) monoclonal antibodies, have shown considerable potential in the treatment of various types of malignancies including melanoma, non-small cell lung cancer, Hodgkin's lymphoma, etc.[12] PD-L1 expressed on both tumor cells and tumor-infiltrating immune cells in the tumor microenvironment is a key immune checkpoint molecule. Binding of PD-L1 to its receptor PD-1 on tumor-specific T cells induces T-cell tolerance and help avoid immune destruction for tumor cells.[13,14] In fact, previous clinical studies demonstrated survival

benefit of PD-1/PD-L1 inhibitors as monotherapy or in combination with other active agent in some of advanced CCRCC patients in clinical studies.[15-19]

In this study, to explore the underlying mechanism of the TKI-resistance regard to upregulation of PD-L1 expression, we analyzed gene expression profile of a total of 10 pairs of metastatic CCRCC (mCCRCC) tissues, which had been harvested at TKI-sensitive pretreatment period and at TKI-resistant post-treatment period. We further investigated signaling pathway associated with the resistant mechanism by bioinformatics data analysis and in vitro studies.

Materials and methods

mCCRCC cases

This study included two cohorts of mCCRCC cases treated with VEGFR-TKIs. As the first discovery cohort to analysis differential gene expression of PD-L1 between TKI-sensitive and TKI-resistant mCCRCC, we retrospectively searched for mCCRCC cases, of which tumor tissues were harvested at not only TKI-sensitive pretreatment period but also TKI-resistant post-treatment period within 3 months of being diagnosed as progressive disease. Among 553 RCC patients who had been treated with VEGFR-TKI at the Asan Medical Center (AMC) from 1997 to 2013, 10 cases satisfied the above criteria and included in the discovery cohort. All specimens were formalin-fixed, paraffin embedded (FFPE).

As a validation cohort, a total of 109 cases of mCCRCC which received VEGFR-TKI were retrospectively collected. Their primary tumor tissues were harvested at initial diagnosis during pretreatment period between 1995 and 2011, formalin-fixed paraffin embedded, and used for tissue microarray (TMA) construct consisting of 2 representative

cores of 1-mm-diameter.

Tumor response to VEGFR-TKI therapy was assessed according to the Revised Response Evaluation Criteria in Solid Tumors (RECIST) guidelines (version 1.1)[20]. Patients with complete or partial response (CR or PR) were considered responders, whereas those with stable or progressive disease (SD or PD) were considered non-responders. Each case had been reviewed and subtyped according to the 2004 World Health Organization (WHO) Tumor Classification; graded according to the Fuhrman grading system; and staged according to the American Joint Committee on Cancer (AJCC) Staging System, 7th edition.[21,22] The 2004 WHO Tumor Classification system and Fuhrman grading system were employed because the cases were examined before the systems proposed.

Gene expression profiling and pathway analysis

Total RNA was extracted from the 10 pairs of pre- and post-treatment FFPE tumor tissues of the discovery cohort. cDNA gene expression profiling analyses were performed using HumanGenome® Human Transcriptome Array 2.0 (Affymetrix, Santa Clara, CA)

according to manufacturers' instruction at an outside laboratory under the supervision of two authors (GHJ and HHS). The raw data were normalized using the robust multiarray average (RMA) method implemented in Transcriptome Analysis Center version 3.0 (Affymetrix, Santa Clara, CA). The probes were annotated using chip files for HTA 2.0 platform for gene set enrichment analysis provided by Broad Institute (http://software.broadinstitute.org/gsea/index.jsp). The differentially expressed genes (DEGs) between PD-L1-expressing and non-expressing groups were investigated by empirical Bayes moderated t-test using R package *limma*.[23] The cut-off criteria for the differentially expressed genes were < 0.05 of normal P-value instead of false discovery rate (FDR) because of the small number of the cases. No annotated genes were excluded.

To find out the enriched pathways for PD-L1 expression, both the hypergeometric test[24] and gene set enrichment analysis (GSEA)[25] were carried out. Hallmark and canonical pathway gene sets (C2cp) of Molecular Signatures Database (MSigDB) version 6.0 (Broad Institute, Cambridge, MA; http://www.broad.mit.edu/gsea/msigdb/index.jsp) were used for the pathway analysis. "Gene set" option was selected permutation type because of the scanty

number of the cases. FDR below 5% was considered for significant enrichment.

Immunohistochemistry

The whole tumor sections of the discovery cohort were assessed for PD-L1 expression. The TMA construct of validation cohort was analyzed for the expression of PD-L1, phospho-Akt (p-Akt), phospho-mammalian target of rapamycin (p-mTOR) and phospho-S6 ribosomal protein (p-S6RP). The primary antibodies used in this study, their dilutions, code and the subcellular location of each antigen are summarized in Table 1. Immunohistochemical (IHC) staining was performed using an automated staining system (BenchMark XT, Ventana Medical Systems, Tucson, AZ, USA) according to the manufacturer's protocol. Nuclei were counterstained with hematoxylin.

IHC staining results were assessed in a semiquantitative manner. The PD-L1 expression was first evaluated according to the intensity (negative, weak, moderate, or strong) and the percentage of positive tumor cells with membranous staining regardless of partial or complete pattern. Then cases with more than weak intensity in >1% of tumor cells were

considered positive for PD-L1 expression. The PD-L1 antibodies for Cell Signaling Technology and Dako were used in discovery cohort and validation cohort, respectively. The expressions of p-Akt, p-mTOR and p-S6RP on TMA slides were first scored based on the percentage of positive tumor cells and the staining intensity (negative, weak, moderate, or strong). Cases with moderate to strong intensity in >5% of tumor cells were regarded as positive. The investigator was blinded to the associated clinicopathological information.

Table 1. Antibodies used in the study

Antibody	Dilution	Code	Company	Subcellular Location
PD-L1 IHC 22C3 pharmDx	-	SK006	Agilent Technologies (Dako), Santa Clara, CA	Membrane
PD-L1	1:100	#13684	Cell Signal Technology, Beverly, MA	Membrane
p-Akt	1:10	#4060	Cell Signal Technology, Beverly, MA	Cytoplasm
p-mTOR	1:100	#2976	Cell Signal Technology, Beverly, MA	Cytoplasm / membrane
p-S6RP	1:100	#2211	Cell Signal Technology, Beverly, MA	Cytoplasm

PD-L1, programmed death-ligand 1; p-Akt, phospho-Akt; p-mTOR, phospho-mammalian target of rapamycin; pS6, phospho-S6 ribosomal protein; PLOD-2, Procollagen-lysine, 2-oxoglutarate 5-dioxygenase 2.

Cell culture

Cell line A human renal cell carcinoma cell line 769-P was purchased from the American Type Culture Collection (ATCC) and cultured in RPMI-1640 medium (Gibco, USA) supplemented with 10% fetal bovine serum (Gibco, USA) and 1% penicillin/streptomycin, at 37 °C in a humidified atmosphere containing 5% CO2.

Resistant cell line development Initially, a dose-response study was performed to analyze drug sensitivity of 769-P to sunitinib (sutent, Pfizer Pharmaceutical, USA). 769-P was treated with sunitinib at various concentrations from 0.1 uM to 50 uM for 72 hours; then 3-(4,5-dimethylthiazol-2-yl)-2,5-diphenyl tetrazolium bromide (MTT) assay was performed as below to estimate IC_{50} value.

To establish sunitinib-resistant 769-P cell line (769-P/suR), 769-P was treated for 6 months with sunitinib at various concentrations ranging from 0.5 uM to 5 uM that was chosen to span the IC_{50} value. Culture medium was changed every 3 days. Sunitinib-sensitive parental 769-P cell line (769-P/suS) was used as control cell line.

MTT assay

Proliferation activity of 769-P cells was evaluated by MTT assay (Sigma Chemical Co., St.Louis, MO). Briefly, Cells ($2x10^4$) at the exponential growth phase were seeded in 96-well plates and allowed to attach overnight at 37°C. After experimental procedures such as sunitinib treatment and transfection assay, MTT reagent was added to each well and incubated for 4 hours at 37°C. The supernatant was discarded; the MTT-formazan crystals formed by metabolically viable cells were solubilized with 100μL of dimethyl sulfoxide (DMSO) on a shaker for 10 seconds; then absorbance was measured in an ELISA microreader at 540 nm.

RNA interference

Small interfering RNAs (siRNAs) for PD-L1 and random negative control (NCT) were purchased from Ambion (Life Technologies, USA) and Invitrogen (Life Technologies,

USA), respectively. The primers of the siRNAs were designed by Primer3 (http://primer3.ut.ee/) based on the open reading frame of the PD-L1 mRNAs. Followings are the siRNA primer sequences: PD-L1, 5′- TTTGCTGTCTTTATATTCATGACC-3′ (forward) and 5′-TCATATTGCTACCATACTCTACCACA-3′ (reverse). The knockdown of PD-L1 expression was validated by quantitative Real-Time PCR and by Western blotting 48 h after transfection. 769-P/suR cells at approximately 70 % confluence were transfected with siRNAs for PD-L1 and NCT at 100 nM and 100 nM, respectively, using Lipofectamine 2000 Reagent (Life Technologies, USA) according to the manufacturer's protocol.

Drugs

Dactolisib (NVP-BEZ235, a dual ATP-competitive PI3K and mTOR inhibitor) and Everolimus (RAD001, mTOR inhibitor) dissolved in DMSO were purchased from KIM & FRIENDS, South Korea and used at a final concentration of 0.5 μM and 5 nM, respectively, by dose-response analysis (data not shown) and based on earlier studies.[26-28]

Quantitative real-time polymerase chain reaction

Total RNA was extracted from cells using TRIzol method, and the aqueous phase obtained after chloroform extraction was subjected to an additional purification step by isopropanol extraction. Total mRNA (300 μg) was reverse transcribed to cDNA using Mir-X miRNA First-Strand Synthesis Kit (TAKARA Biotechnology, Japan) and diethyl pyrocarbonate (DEPC)-treated water was added to the obtained cDNA for dilution and complete mixing. Quantitative real-time polymerase chain reaction (qRT-PCR) was performed using ABI 7500 Real-Time PCR System (Applied Biosystems, Foster City, California, USA) according to the manufacturer's instructions. The total reaction volume was 20 μl and consisted 10 μl of SYBR Premix Ex Taq™, 2 μl of cDNA, 6.8 μl of DEPC water, 0.4 μl of ROX reference dye and 0.4 μl each of the forward and reverse primers. β-actin was used as an internal control, the relative expression of target gene was calculated

using the CT ($2^{-\Delta\Delta CT}$) method, and the results were statistically analyzed. The experiments were performed at least three times.

Specific primers were as follows: PD-L1, 5'- TTGGGAAATGGAGGATAA -3' (forward) and 5'- GGATGTGCCAGAGGTAGTTCT -3' (reverse); β-actin, 5'- CCATCGTCCACCGCAAA -3' (forward) and 5'- TCAAGAAAGGGTGTAACGCAACTA -3' (reverse).

Western blotting

Whole cell extracts were prepared using RIPA lysis buffer (89900; Thermo scientific, USA) and protease inhibitor cocktail (BPI-9200; Tech & Innovation Co, Korea). The concentration of protein was quantified with the Bradford Method using a commercial kit (Bradford Protein Assay, Bio-Rad, USA), purchased from the Bio-Rad Laboratories. Total protein was subjected to electrophoresis on 12 % (PD-L1, p-S6RP, and p-AKT) and 8% (p-mTOR) of sodium dodecyl sulfate-polyacrylamide gel electrophoresis (SDS-PAGE) gels for

2 hours at 80V, transferred to polyvinylidene difluoride (PVDF) membranes, then blocked with 5% skim milk or bovine serum albumin (BSA). Primary antibodies were then added, followed by overnight incubation in a rotator at 4˚C. After washing three times with Tris-HCl buffer solution-Tween (TBST), the membrane was treated with a horseradish peroxidase (HRP)-conjugated secondary antibody at room temperature for 1 hour. Then, the membrane was washed three times with TBST in the same manner, and enhanced chemiluminescence (ECL) (Thermo scientific, USA) was added to detect the protein bands. Films were washed with pure water after development and dried for scanning and recording.

The PD-L1 antibody obtained from Cell Signaling Technology was used for western blotting. The other primary antibodies were the same ones used for immunohistochemistry. β-actin was served as the internal control.

Clonogenic survival assay

Cells were plated onto six-well plates in triplicate at 0.5×10^3 cells per well and incubated in RPMI 1640 with 10% FBS at 37°C. After 2 weeks in culture, colonies were stained with 1.0% crystal violet for 15 minutes, then grossly visible colonies were counted manually. Clonogenic surviving point (SP) was calculated as follows: SP = (number of colonies formed at a given dose/number of cells plated at a given dose) x (control number of cells plated/control number of colonies formed).[29]

Wound healing assay

Cells were plated onto six-well plates at 8×10^5 cells in triplicate and incubated in RPMI 1640 with 10% FBS at 37°C. After overspreading on the plate, cells were wounded by drawing vertical scratches with a plastic pipette tip, and incubated in regular medium. Migration of cells was observed and photographed under optical microscope regularly up to 40 hours.

Matrigel invasion assay

A total of 100μl of serum-free medium including matrigel was added to each well of a 24-well plate containing inserts with 8 μm pores and incubated overnight at 37°C to form an artificial basement membrane. Then 2.5×10^5 cells were seeded in triplicate on the upper chamber of transwell and media containing 10% FBS were added into the lower chamber. Following 48 hours incubation at 37°C, cells remaining on the top of inserts in upper membrane were wiped with cotton swab, while cells migrated or invaded underside of membrane were fixed in 3.7% formaldehyde, then stained with 1% crystal violet. Cells penetrated matrigel were photographed.

Statistical analysis

For descriptive statistics, all continuous data were expressed as mean ± standard deviation (SD) or median value. All categorical data were compared with the chi-square test. p-value of <0.05 were considered statistically significant.

Results

Patient characteristics

The clinicopathological features at initial diagnosis and at progressed disease of the 10 cases of the discovery cohort are summarized in Table 2. In 10 pairs of pre- and post-treatment tumor tissues, the median age was 51.8 years (range, 40–66 years) with a 4:1 male/female ratio. The mean tumor size was 10.1 cm in its greatest dimension (range, 2.5–21.0 cm). Two cases had undergone percutaneous needle biopsy whereas the others had undergone radical nephrectomy or resection before the TKI treatment. One case who underwent nephrectomy was operated by an outside hospital so that some of the clinical data were not available. Most of tumors were high-grade (Fuhrman grades 3 or 4: 7/9 cases) and high-stage (pT3 and pT4, 8/10 cases). Three cases had metastasis at the time of initial diagnosis (3/10 cases) with 2 months of median period to metastasis (range, 0-169 months). The lung was the most common metastatic site (7/10 cases).

In 10 pairs of pre- and post-treatment tumor tissues at progressed disease after

using VEGFR-TKI treatment, 2 cases had undergone percutaneous needle biopsy whereas the others had undergone excision. The metastatic sites where they had undergone procedure were intestine and mesentery (3 cases), lung (2 cases), abdominal wall (1 case), thigh (1 case), scalp (1 case), brain (1 case) and stomach (1 case). The rates of Fuhrman grade 4 (4 cases versus 6 cases) and sarcomatoid features (3 cases versus 6 cases) were higher than at the time of initial diagnosis.

Four patients received other treatments prior to VEGFR-TKI treatment, which were interferon (2 cases), interleukin-2 (1 case) and radiotherapy (1 case). Seven cases received sunitinib and three cases pazopanib with 3.5 months of median treatment time (range, 1-194 months). All of the patients were eventually died of the disease with rate 50 months of median survival period (range, 7-221 months) after initial diagnosis and 24.5 months (range, 5-96 months) after starting the VEGFR-TKI treatment.

Table 2. Clinicopathologic features of 10 pairs of metastatic clear cell renal cell carcinoma cases of discovery cohort

Variables		Case number									
		1	2	3	4	5	6	7	8	9	10
Age	Years	56	54	42	53	54	66	40	53	45	55
Sex	Male / female	Male	Male	Male	Female	Male	Female	Male	Male	Male	male
Primary tumor at initial diagnosis	Fuhrman nuclear grade*	3	-	2	4	4	3	1	4	4	3
	pT stage	3	3	3	4	3	3	1	1	4	3
	Tumor size (cm)	7	-	16	8.5	11	9	7	2.5	21	9
	Lymphovascular invasion*	Present	-	Present	Present	Absent	Absent	Absent	Absent	Present	Absent
	Perirenal fat invasion	Absent	Present	Present	Present	Absent	Present	Absent	Absent	Present	Present
	Renal sinus fat invasion*	Present	-	Absent	Present	Present	Absent	Absent	Absent	Present	Absent
	Direct extension to the adrenal gland	Absent	Absent	Absent	Present	Absent	Absent	Absent	Absent	Absent	Absent
	Necrosis (%)	0	-	0	30	15	Absent	0	5	30	0
	Sarcomatoid feature (%)	0	-	0	5	0	0	0	50	80	0
	Lymph node metastasis	Absent	Absent	Absent	Absent	Absent	Absent	Absent	Absent	Present	Absent
	procedures	Resection	Resection	Resection	Resection	Resection	Biopsy	Resection	Resection	Resection	Biopsy
	Initial metastasis	Yes	No	No	Yes	No	Yes	No	No	No	No
	Initial sites of metastasis	Lung, pelvic bone	Lung	Lung	Lung	Lung	Lung, pancreas	Cheek	Spinal bone	Ileum	Lung, pancreas, leg
Tumor at progressed disease	Fuhrman nuclear grade	2	1	3	4	4	4	3	4	4	4
	Necrosis (%)	0	0	0	80	0	0	5	0	5	0
	Sarcomatoid feature (%)	5	0	0	40	60	60	0	80	95	0
	Procedures	Resection	Resection	Resection	Resection	Resection	Resection	Resection	Biopsy	Resection	Biopsy
	Metastatic sites of procedure	Ileum and mesentery	Scalp	Lung	Both intestines	Brain	Stomach	Thigh	Abdomina -l wall	Ileum	Lung
TKI regimen	Sunitinib / pazopanib	Sunitinib	Sunitinib	Sunitinib	Sunitinib	Pazopanib	Sunitinib	Pazopanib	Sunitinib	Pazopanib	Sunitinib
Prior immune or/and cytotoxic therapy		No	Interferon	No	No	No	No	No	Radiation therapy	Interferon	Interleukin -2
Follow-up period	Months	13	150	167	11	43	57	221	27	7	143
Cancer-related death		Yes	Yes	Yes	Yes	Yes	Yes	Yes	Yes	Yes	Yes
Time from diagnosis to TKI initiation	Months	1	61	71	2	4	1	194	3	2	132

Time from diagnosis to distant metastasis	Months	0	29	70	0	1	0	169	1	3	123
Time to death from TKI initiation	Months	12	89	96	8	39	55	26	23	5	10

SD, standard deviation; TKI, Tyrosine kinase inhibitor.

* Because case number 2 was undergone radical nephrectomy at an outside hospital, some of the clinical data were not available.

Expression of PD-L1 in a small proportion of VEGFR-TKI resistant CCRCC

Global gene expression was compared by cDNA microarray using paired tumor tissues of the 10 cases of discovery cohort harvested at TKI-sensitive pretreatment status and TKI-resistant progressed status after the TKI treatment. Among differentially expressed genes, microarray fold change of PD-L1 was elevated at mRNA level in four cases (case 1, 3, 4 and 10) in post-treatment tissues compared to pre-treatment ones (Table 3. and Fig. 1A-1B).

To verify the microarray results at protein level, PD-L1 IHC staining was performed. Pretreatment and posttreatment tissues were available for PD-L1 IHC staining in 7 cases after the usage of tumor tissues for the microarray experiment (Fig. 1C). In two cases (case 3 and case 10) whose PD-L1 mRNA was increased in the posttreatment tissue, PD-L1 expressing tumor cells was increased from none in pretreatment tissues to 100% and 100%, respectively, in posttreatment tissues (Fig. 1D). Although expression of PD-L1 was also observed in case 4, it was false positive expression because it showed a cytoplasmic pattern rather than a membranous pattern. The slight elevation of fold change in case 1 was not considered to be significant in correlation with PD-L1 expression of protein level.

Accordingly, two of three cases (case 3 and case 10) did recapitulate its mRNA result.

These results demonstrate that PD-L1 expression was increased in a small proportion of TKI-resistant CCRCC cases.

Table 3. Value of microarray raw data and fold change of PD-L1 (CD274) per each case in 10 pairs of pre- and posttreatment metastatic clear cell renal cell carcinoma tissues of discovery cohort

Case number	Pretreatment	Posttreatment	Log_2FC	FC
1	3.900	3.963	0.063	1.044
2	3.990	3.907	-0.083	0.944
3	3.989	4.605	0.616	**1.533**
4	3.918	4.184	0.265	**1.202**
5	4.247	4.044	-0.203	0.869
6	3.866	3.777	-0.089	0.940
7	3.998	3.924	-0.074	0.950
8	4.073	4.055	-0.018	0.987
9	3.836	3.657	-0.179	0.883
10	3.560	3.832	0.272	**1.207**

TKI, Tyrosine kinase inhibitor; FC, Fold change.

A

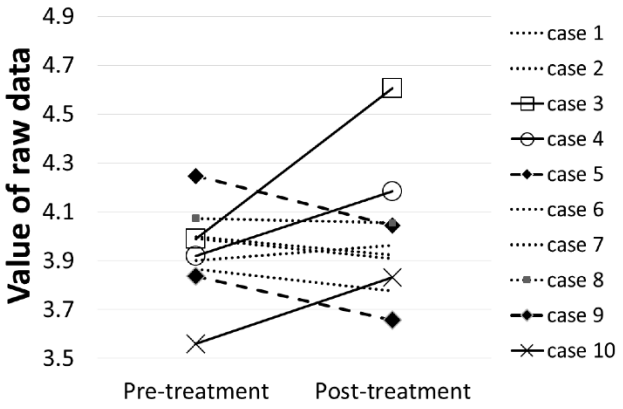
Value of raw data
4.9
4.7
4.5
4.3
4.1
3.9
3.7
3.5
Pre-treatment
Post-treatment
case 1
case 2
case 3
case 4
case 5
case 6
case 7
case 8
case 9
case 10

B

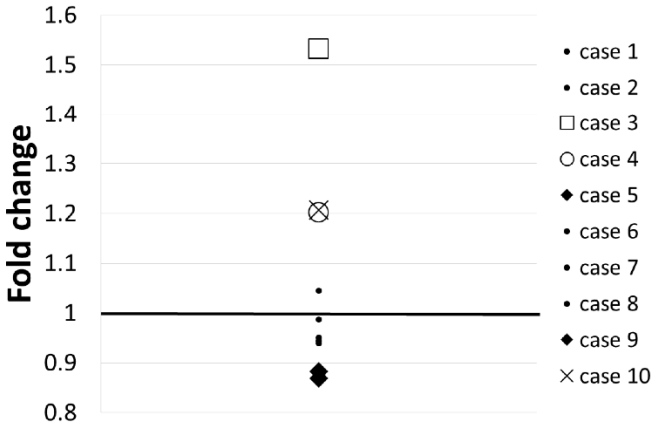
Fold change
1.6
1.5
1.4
1.3
1.2
1.1
1
0.9
0.8
case 1
case 2
case 3
case 4
case 5
case 6
case 7
case 8
case 9
case 10

C

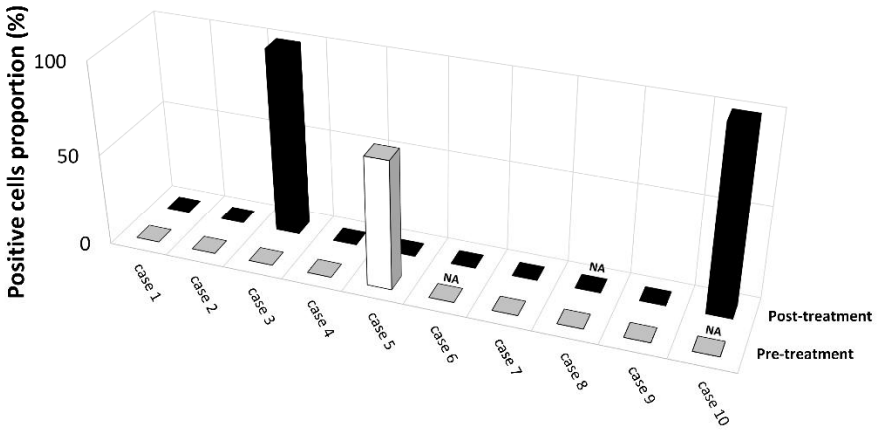
Positive cells proportion (%)
100
50
0
case 1
case 2
case 3
case 4
case 5
case 6
case 7
case 8
case 9
case 10
NA
NA
NA
Post-treatment
Pre-treatment

D

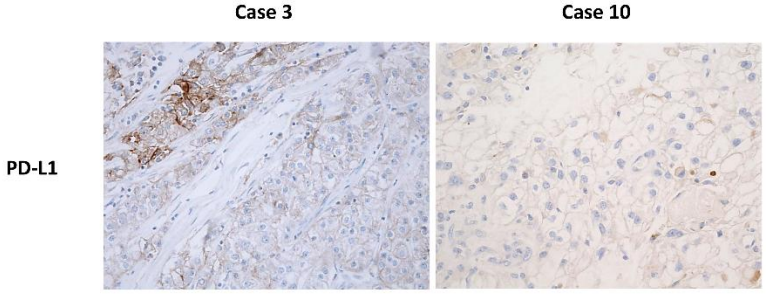
Case 3
Case 10
PD-L1

Figure 1 Value of microarray raw data and fold change of the 10 cases of discovery cohort and validated results of PD-L1 IHC staining. **(a, b)** Value of microarray raw data and fold change of TKI-resistant posttreatment period in case 3, 4 and 10 are more increased than TKI-sensitive pretreatment period in 10 pairs of mCCRCC tissues. Case 1 was not included in the increased group because it was not considered to be significant elevation in correlation with PD-L1 expression of protein level. **(c)** Two of three cases whose PD-L1 mRNA was increased in the posttreatment tissue (case 3 and 10) for PD-L1 IHC staining are more increased than TKI-sensitive pretreatment period in 10 pairs of mCCRCC tissues. Tissues of cases 6 and 10 of pretreatment, and of case 8 of posttreatment were all biopsy tissues and could not be confirmed because of insufficient quantity to perform IHC staining. NA; not available. **(d)** Representative images for PD-L1 expression in TKI-resistant posttreatment period of case 3 and 10 by IHC staining.

Analyses of global gene expression and pathway associated with PD-L1 upregulation

To define genes associated with PD-L1 upregulation, global gene expression of three cases whose PD-L1 mRNA levels increased were compared to those of remaining seven cases. When the selection criteria of < 0.05 of normal P-value was applied, all 434 DEGs were obtained.

To define genetic pathways associated with the PD-L1 upregulation, hypergeometric test was performed by applying DEGs with FDR < 5% to C2cp gene sets and hallmark gene sets which were refined and classic. The results showed that the DEGs were significantly associated with 14 signaling pathways (Table 4). When the DEGs were applied on GSEA using hallmark gene set, 26 gene sets were significantly enriched (Table 5). mTOR complex 1 signaling, hypoxia, and glycolysis were selected in common by both hypergeometric test and GSEA. Since mTOR inhibitors has been widely used to treat advanced RCC patients, mTOR complex 1 signaling pathway was chosen to study further (Fig. 2A).

mTOR complex 1 associated genes (GBE1, PLOD2, HSPA9, PDAP1, HSPA5, NMT1, PSMC2, TES, ACLY and HSPD1) were identified to be overlapped between DEGs which obtained by comparing the PD-L1 upregulated three cases with the remaining seven cases at mRNA level and hallmark mTOR complex 1 gene sets of GSEA. The figure 2B demonstrated the mTOR complex 1 associated genes and selected 10 DEGs which applying more stringent criteria of absolute value of log-fold change > 1 (Supplementary table 1) in two groups divided by upregulation of PD-L1.

Furthermore, mTOR complex 1 associated genes (PLOD2, SYTL2, NAMPT, SLC7A5, HSPA9, BHLHE40, ATP2A2, LDHA, ACLY, EIF2S2, CALR, CDKN1A, HSPA5 and SLC2A1) were identified to be overlapped between the 561 DEGs which obtained by comparing the PD-L1 upregulated three cases with the PD-L1 downregulated two cases (case 5 and case 9) at mRNA level in posttreatment tissues (Fig. 1A and 1B) and hallmark mTOR complex 1 gene sets of GSEA (Table 6).

These results suggested that PD-L1 expression of TKI-resistant CCRCC cases was associated with the mTOR pathway activation.

Table 4 Selected signaling pathway for pathway analysis using hypergeometric test

Pathway names	Pathway description	Length	Overlap	p-value	FDR
Glycolysis	Conversion of glucose into pyruvate	200	80	0.000092	0.016
Hypoxia	The regulation of oxygen homeostasis	200	9	0.000013	0.006
mTOR C1 signaling	The regulation of cell growth and survival in response to nutrient and hormonal signals	200	10	0.000001	0.001
Starch and sucrose metabolism	Carbohydrate metabolism	52	5	0.000032	0.010
Integrin 3 pathway	Cell adhesion and cell surface mediated signaling	43	4	0.000238	0.027
UPA Upar pathway	Localizing and promoting plasmin formation	42	4	0.000217	0.027
Calnexin calreticulin cycle	Binding to oligosaccharides and targeting them for degradation	11	3	0.000054	0.012
Glucuronidation	Catalyze a wide range of diverse endogenous and xenobiotic compounds	18	3	0.000260	0.027
Integrin alpha IIb/beta 3 signaling	Signaling in platelet adhesion and aggregation	27	4	0.000037	0.010
Integrin cell surface interactions	Mediation of cell adhesion to ECM	79	7	0.000001	0.001
N glycan trimming in the ER and calnexin Caleticulun cycle	Mediation of folding of protein	13	3	0.000093	0.016
Platelet aggregation plug formation	Formation of a platelet thrombus	36	4	0.000118	0.016
Insulin receptor pathway in cardiac myocytes	The regulation of glucose homeostasis	51	4	0.000462	0.045
PIP3 signaling in cardiac myocytes	Activation in cardiac myocyte by the receptors with intrinsic tyrosine kinase activity	67	5	0.000112	0.016

mCCRCC, Metastatic clear cell renal cell carcinoma; TKI, Tyrosine kinase inhibitor; LogFC, log-fold change; mTOR C1, phospho-mammalian target of rapamycin complex-1; UPA, Urokinase-type plasminogen activator; Upar, Urokinase plasminogen activator receptor; PIP3, Phosphatidylinositol (3,4,5)-trisphosphate; ECM, extra cellular matrix.

Table 5. Selected signaling pathway for pathway analysis using gene set enrichment analysis

Pathway names	Pathway description	Size	p-value	FDR q-value
Glycolysis	Conversion of glucose into pyruvate	188	0	0
Hypoxia	The regulation of oxygen homeostasis	195	0	0
mTOR C1 signaling	Regulation of cell growth and survival in response to nutrient and hormonal signals	192	0	0.0006
Adipogenesis	Fat cells differentiate from preadipocytes to adipocytes	193	0	0.0220
Androgen response	The growth and development of the male reproductive organs	98	0	0
Angiogenesis	The transcription of VEGF1, FGF2, PDGF-beta, MMP9, MMP2 and Ang1 for vessel formation	32	0	0
Apical junction	Providing the paracellular barrier, contributing to maintenance of the apical–basal cell polarity and providing a site for signaling	188	0	0.0016
Apoptosis	Acting in a proteolytic cascade to dismantle and remove the dying cell	155	0	0.0017
Cholesterol homeostasis	Controlling the cholesterol level	71	0	0.0006
Coagulation	Leading to fibrin formation	133	0	0
Complement	Activation of the complement system	191	0.004	0.0233
Epithelial mesenchymal transition	Epithelial cells gain properties to become mesenchymal stem cells	190	0	0
Estrogen response early	The growth and development of the female reproductive organs	195	0	0
Estrogen response late	The growth and development of the female reproductive organs	191	0	0.0042
Hedgehog signaling	Transmits information to embryonic cells required for proper cell differentiation	35	0.004	0.0045
IL-2 STAT5 signaling	Shaping the development of both natural and induced regulatory T cells	196	0	0.0211
Inflammatory response	The activation of inflammatory response	199	0.002	0.0273
KRAS signaling up	The activation of KRAS signaling pathway	195	0	0.0006
Myogenesis	Formation of muscular tissue	193	0.002	0.0192
P53 pathway	Tumor suppressor activating the major apoptosis signaling pathway	192	0	0.0017
Protein secretion	The process of protein synthesis in endoplasmic reticulum and transport of proteins to the cell organelles	92	0.010	0.0156
TGF-beta signaling	The regulation of wide spectrum of cellular function such as proliferation, apoptosis, differentiation and migration	53	0	0
TNF-alpha signaling via NF-κB	The regulation of a wide spectrum of biological processes including cell proliferation, differentiation, apoptosis, lipid metabolism, and coagulation.	193	0	0.0002
Unfolded protein response	Cellular stress response related to the endoplasmic reticulum stress	106	0	0.0005
UV response	DNA damage and cell proliferation arrest	138	0	0
Xenobiotic metabolism	The metabolism of foreign substances affecting to the human body	192	0	0.0016

mTOR C1, mTOR complex 1; VEGF1, Vascular endothelial growth factor1; FGF2, fibroblast growth factor 2; PDGF-beta, Platelet-derived growth factor-beta; MMP9, Matrix metallopeptidase 9; MMP2, Matrix metallopeptidase 2; IL-2, Interleukin-2; STAT5, Signal transducer and activator of transcription 5; TGF-beta, Trans forming growth factor-beta; TNF-alpha signaling via NF-κB, Tumor necrosis factor-alpha signaling via nuclear factor kappa-light-chain-

enhancer of activated B cells.

Table 6. Selected signaling pathway for pathway analysis comparing the PD-L1 upregulated three cases with the PD-L1 downregulated two cases by gene set enrichment analysis

Pathway_names	Associated genes	FDR q-value
mTOR C1 signaling	**PLOD2, SYTL2, NAMPT, SLC7A5, HSPA9, BHLHE40, ATP2A2, LDHA, ACLY, EIF2S2, CALR, HSPA5, CDKN1A, SLC2A1**	0.000005
Glycolysis	VCAN, PLOD2, MET, FAM162A, ENO2, LDHA, HSPA5, CD44	0.043442
Hypoxia	WSB1, FAM162A, ENO2, CA12, BHLHE40, NDRG1, LDHA, CDKN1A, HSPA5, SLC2A1	0.006446
Epithelial mesenchymal transition	VCAN, PLOD2, LRP1, POSTN, TFPI2, ENO2, CDH11, ACTA2, TNFRSF12A, CDH6, IGFBP4, CALD1, CD44, THBS1	0.000005
HIF1-TF	BHLHE40, CA9, NDRG1, LDHA, HIF1A, SLC2A1	0.006446
Nitrogen metabolism	GLS, GLUD2, CA12, CA9	0.007250
Smooth muscle contraction	ITGA1, ACTA2, CALD1, MYL6B	0.008734
Calnexin calreticulin cycle	GANAB, PDIA3, CALR	0.010776
Inflammatory response	MET, SRI, CCL7, NAMPT, OLR1, GPR183, ATP2A2, HIF1A, CDKN1A	0.014183
N glycan trimming in the ER and calnexin calreticulin cycle	GANAB, PDIA3, CALR	0.014713
HIF	LDHA, P4HB, HIF1A	0.020953
Angiogenesis	VCAN, POSTN, APP, OLR1	0.021689
Unfolded protein response	SEC31A, SLC7A5, HSPA9, CALR, HSPA5, IARS	0.043442
Antigen presentation folding assembly and peptide loading of class Ⅰ MHC	SEC31A, PDIA3, CALR, HSPA5	0.006446
Muscle contraction	ITGA1, ACTA2, CALD1, MYL6B	0.049572
Asparagine N limked glycosylation	SEC31A, GANAB, PDIA3, CALR, DAD1	0.049572

mTOR C1, mTOR complex 1; HIF, Hypoxia-inducible factors; TF, Tissue factor; ER, Endoplasmic reticulum; MHC, Major histocompatibility complex.

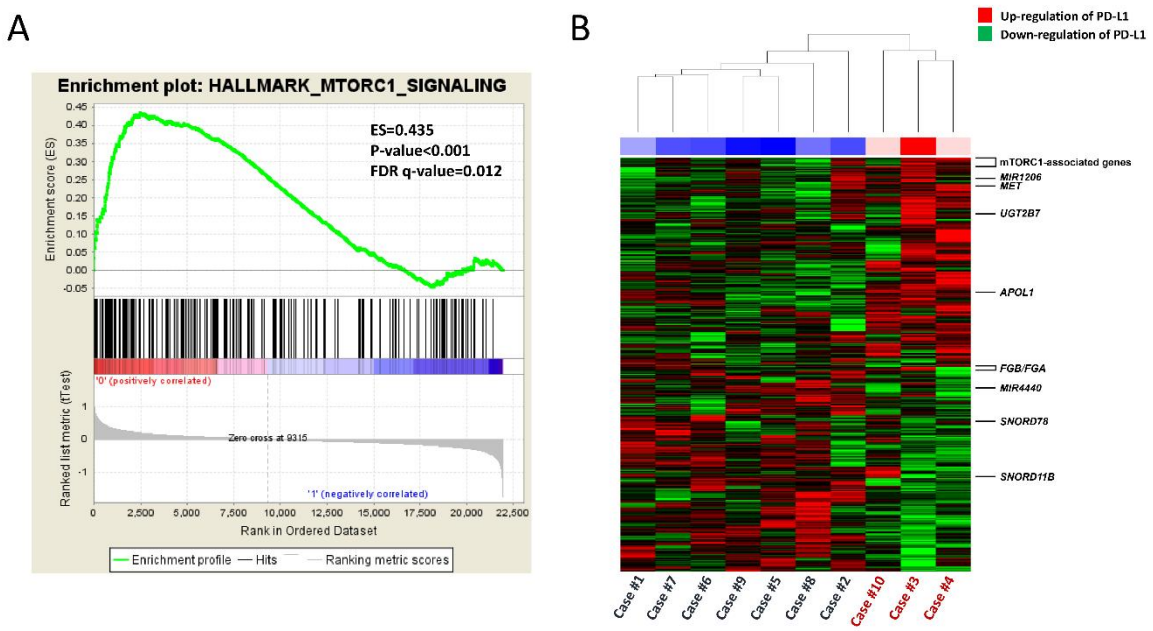

Figure 2 Enrichment result for the 'Hallmark mTOR C1 signaling' gene set from the Gene Set Enrichment Analysis of microarray data from two groups with different expression of PD-L1 after VEGFR-TKI treatment of mCCRCC. **(a)** GSEA using Affymetrix gene expression data from two groups with different expression of PD-L1 after VEGFR-TKI treatment of mCCRCC found significant (FDR q-value=0.012) enrichment of a set of genes dependent in hallmark mTOR C1 signaling. The enrichment score is calculated by walking down a list of genes ranked by their correlation with the up-regulated PD-L1 expression, increasing a running-sum statistic when a gene in that gene set is encountered (each black vertical line underneath the enrichment plot) and decreasing it when a gene that isn't in the gene set is encountered. The enrichment score is the maximum deviation from zero encountered in the walk. **(b)** Heat map overview of levels of mTOR complex 1 associated genes (PLOD2, SYTL2, NAMPT, SLC7A5, HSPA9, BHLHE40, ATP2A2, LDHA, ACLY, EIF2S2, CALR, CDKN1A, HSPA5 and SLC2A1; Individual gene names did not appear.) and selected 10 genes including seven genes up-regulated (APOL1, FGA, FGB, MET, MIR1206, PLOD2 and UGT2B7) and three genes down-regulated (MIR4440, SNORD11B and SNORD78) across two groups with different expression of PD-L1 after VEGFR-TKI treatment of mCCRCC. Shades of red

and green represent elevated and reduced levels of genes, respectively (see color scale).

Supplementary table 1. Selected 10 genes with absolute value of log-fold change > 1 in the PD-L1 upregulated cases

Probe set ID	Gene symbol	Gene title	Regulation
TC01003533.hg.1	SNORD78	small nucleolar RNA, C/D box 78	Down regulated
TC02001190.hg.1	SNORD11B	small nucleolar RNA, C/D box 11B	Down regulated
TC02002923.hg.1	MIR4440	microRNA 4440	Down regulated
TC03001866.hg.1	PLOD2	procollagen-lysine, 2-oxoglutarate 5-dioxygenase 2	Up regulated
TC04000371.hg.1	UGT2B7	UDP glucuronosyltransferase 2 family, polypeptide B7	Up regulated
TC04000777.hg.1	FGB	fibrinogen beta chain	Up regulated
TC04001662.hg.1	FGA	fibrinogen alpha chain	Up regulated
TC07000722.hg.1	MET	met proto-oncogene (hepatocyte growth factor receptor)	Up regulated
TC08000754.hg.1	MIR1206	microRNA 1206	Up regulated
TC22000265.hg.1	APOL1	apolipoprotein L 1	Up regulated

Association of mTOR signaling pathway with PD-L1 upregulation in CCRCC treated with TKI

To validate the gene set analyses results, expressions of PD-L1 and mTOR signaling pathway were assessed by immunohistochemistry on the validation cohort of mCCRCC. The brief clinicopathological features of the validation cohort are summarized in supplementary table 2.

p-Akt, p-mTOR, and p-S6RP were assessed as mTOR signaling pathway-related proteins. The PD-L1 IHC 22C3 pharmDx antibody obtained from Agilent Technologies (Dako) was used on validation cohort of CCRCC TMA tissues (Fig. 3). PD-L1 expression was positive in 16 cases (14.7%) in 109 cases of validation cohort and was positively correlated with the expression of p-S6RP (p=0.004), which been used as a surrogate for mTORC1 activity[30,31] although it was not correlated with expression of p-mTOR (p=1.000) (Table 7). Therefore, these results suggested that PD-L1 expression was increased in some cases in VEGFR-TKI resistant CCRCC and it was associated with activation of mTOR pathway.

Table 7. Correlation between expression of phospho-S6 ribosomal protein and expression of PD-L1 in 109 cases of validation cohort

		PD-L1, n (%)		
		Negative (n=93, 85.3%)	Positive (n=16, 14.7%)	p-value
p-S6RP	Negative (n=70, 64.2%)	65 (69.9)	5 (31.3)	**0.004**
	Positive (n=39, 35.8%)	28 (30.1)	11 (68.7)	

PD-L1, programmed death-ligand 1; p-S6RP, phospho-S6 ribosomal protein.

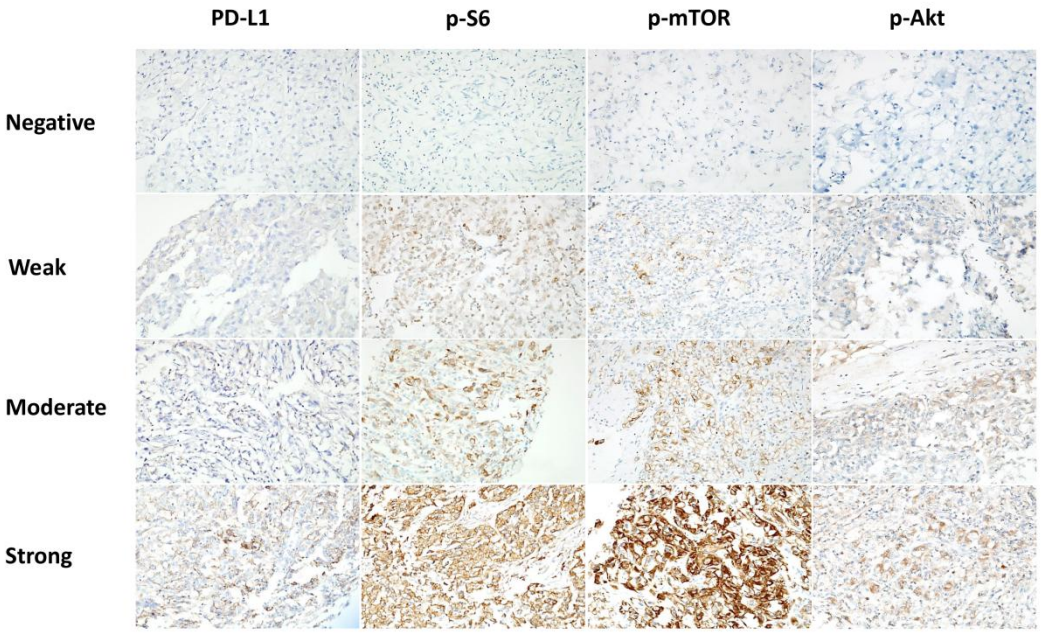

Figure 3 Representative images from the immunohistochemical analysis for PD-L1 (Dako), p-S6RP, p-mTOR and p-Akt according to the intensity.

Supplementary table 2. Clinicopathologic features of 109 cases of metastatic clear cell renal cell carcinoma cases of validation cohort

Variables		Value, n (%)
Age (years)	Mean ± SD	57.3±10.8
Sex	Male	78 (71.6)
	Female	31 (28.4)
Fuhrman nuclear grade	2	19 (17.5)
	3	42 (38.5)
	4	48 (44.0)
Necrosis	Present	61 (56.0)
	Absent	48 (44.0)
Sarcomatoid feature	Present	48 (44.0)
	Absent	61 (56.0)
Responsiveness to TKI treatment	Response	43 (39.4)
	Non-response	66 (60.6)
Disease progression	Yes	90 (82.6)
	No	19 (17.4)
Cancer-related death	Yes	85 (78.0)
	No	24 (22.0)
Follow-up period (m)	Mean (range)	55.9 (2-220)
Time from diagnosis to distant metastasis (m)	Mean (range)	17.4 (0-156)

Progression-free survival analysis of PD-L1 expression in two groups with different TKI responsiveness

The validation cohort consisted of 109 cases, which was classified into 43 cases in the responder group (39.4%) and 66 cases in the non-responder group (60.6%) according to the RECUST criteria (Supplementary table 2). The TKI-non-responder group showed higher expression of PD-L1 in tumor cells compared to responder group, but there was insignificant difference (18.2% versus 9.3%, p=0.272).

As shown in Figure 4, PD-L1 immunopositivity showed statistical insignificant difference relating to progression-free survival (PFS) in responder group (p=0.240), but was associated with shorter PFS in non-responder group (p=0.03). Therefore, PD-L1 expression is a prognostic indicator for poor PFS in patients with mCCRCC receiving TKI treatment.

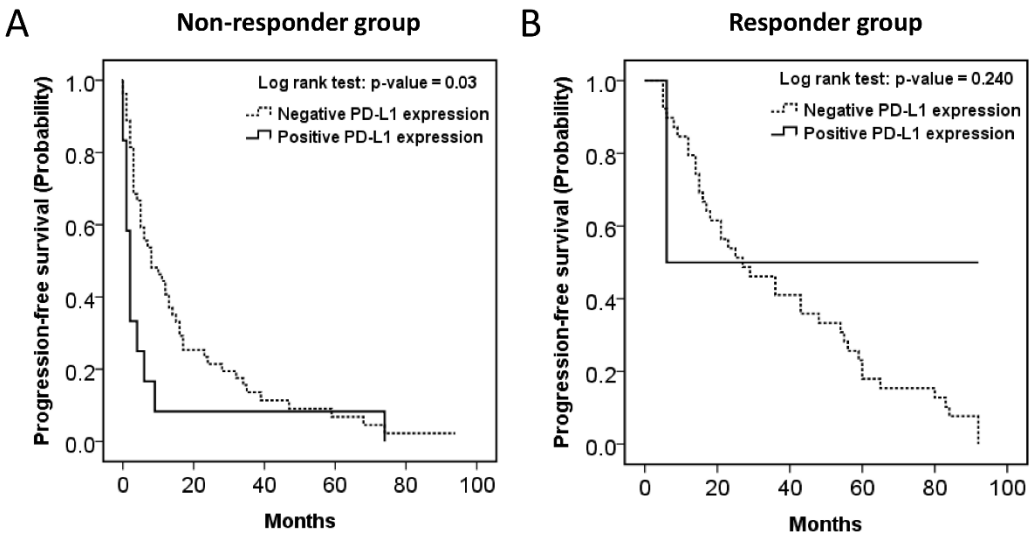

Figure 4 Kaplan-Meier analysis of PD-L1 expression in two groups with different TKI responsiveness. **(a)** Progression-free survival (PFS) rates were lower in patients showing PD-L1 immunopositivity compared to those showing PD-L1 immunonegativity in non-responder group. **(b)** PFS rates were not associated with PD-L1 immunopositivity in responder group.

Development of VEGFR-TKI resistant CCRCC cell line with PD-L1 upregulation

To undergo functional studies related to TKI-resistance, TKI-resistant CCRCC cell lines were developed by long term treatment of five RCC cell lines, 769-P, 786-O, A704, ACHN, and Caki-1 with sunitinib. Among the five cell lines, 769-P was successfully established sunitinib resistance with increased PD-L1 expression in the resistant cells as described below. The expressions of PD-L1 at the protein level of each of the five sunitinib sensitive (suS) and sunitinib resistant (suR) cell lines were demonstrated in the Figure 5A.

The VEGFR-TKI resistance was examined by treating 769-P cell line, which had been cultured with 0.5, 1.5, 2.5 or 5 uM of sunitinib for 6 months, with various concentration of sunitinib. As shown in Figure 5B, the half maximal inhibitory concentration (IC_{50}) of 769-P treated with 0.5, 1.5, 2.5 and 5 uM sunitinib sub-lines were 15, 15.4, 15.5 and 17.7 μM, respectively, whereas that of 769-P/suS was 10 μM. Therefore, 769-P cells treated with 5 uM was chosen for further functional studies regarding TKI-resistance and designated as 769-P/suR.

As shown in Figure 5, there was significant upregulation of PD-L1 at the mRNA

level (p=0.005, Fig. 5C) and at the protein level (Fig. 5A) in the 769-P/suR compared to the 769-P/suS.

Characteristics of sunitinib-resistant 769-P cells

In addition to the TKI resistant high proliferative capacity (Fig. 5B), 769-P/suR showed larger numbers and sizes of colonies compared to 769-P/suS in the colony-forming assay, suggesting that 769-P/suR has higher clonogenic survival than 769-P/suS (Fig. 5D). Survival point was 34. The abilities of the 769-P/suR on invasion and migration were determined using the matrigel invasion assay and scratch test assay, respectively. The number of cells of 769-P/suR that invaded underside of matrigel membrane and migrated into the scratched area were increased compared to the 769-P/suS (Fig. 5E and 5F). These results suggest that 769-P/suR have acquired aggressive behaviors including proliferation, invasion and migration of cancer cells.

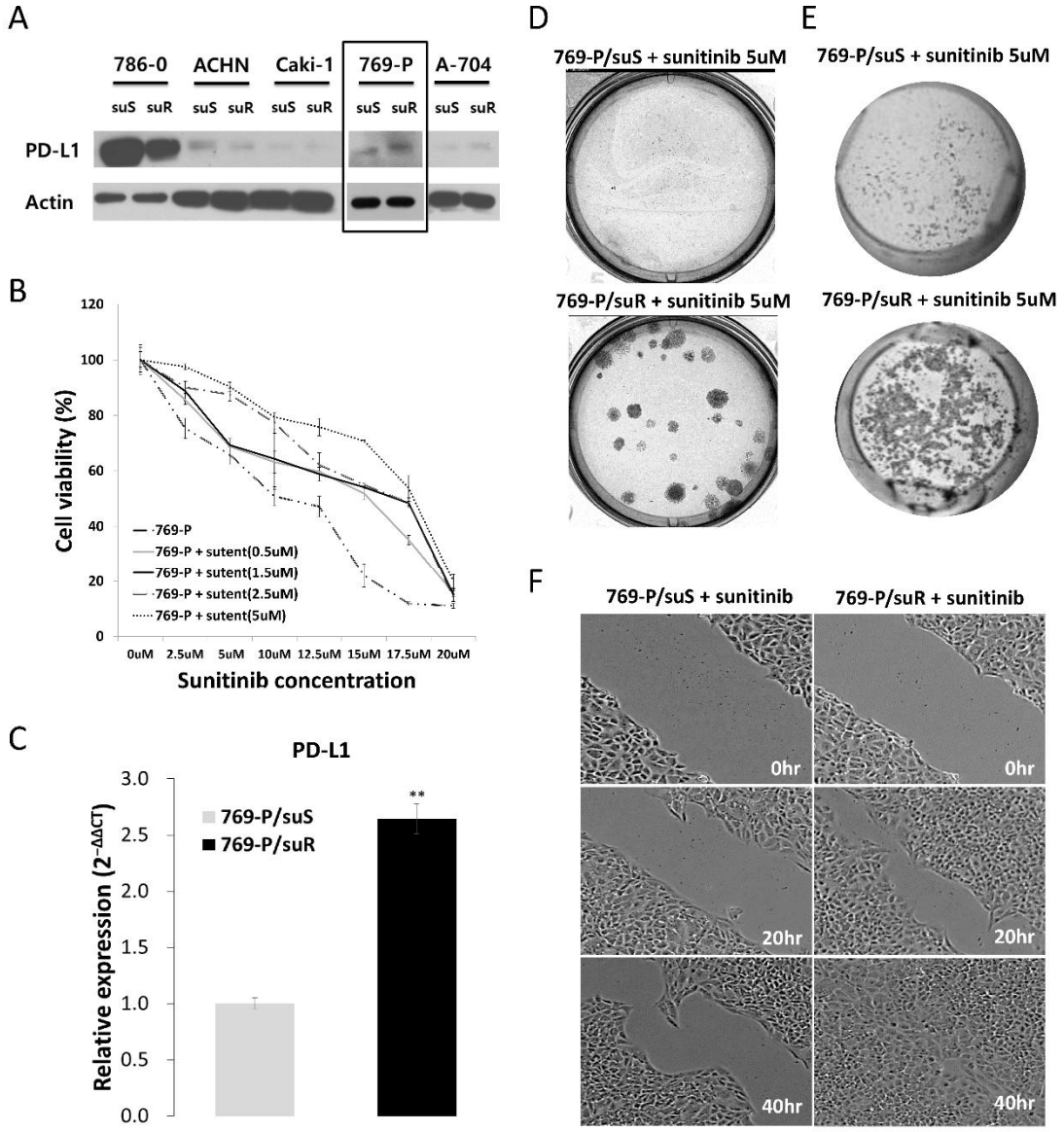

Figure 5 Development of 769-P/suR with PD-L1 expression and increase aggressive tumoral behavior. **(a)** The expressions of PD-L1 at the protein level of each of the five sunitinib sensitive and sunitinib resistant cell lines. 769-P was successfully established sunitinib resistance with increased PD-L1 expression. **(b)** 769-P/suS and 769-P/suR were treated with sunitinib at the indicated concentration, and the relative cell viability was determined by MTT assay. 769-P cells treated with 5 uM was chosen for further studies. **(c)** Up-regulation of PD-L1 expression at the mRNA level in 769-P/suR compared to 769-P/suS by qRT-PCR Data shown in (c) are based on the mean ± SD and *p* value was obtained using Student's t test. $p < 0.05$ is indicated by "**". **(d)** Proliferative capacity of 769-P/suS and 769-P/suR

was assessed using colony formation assay. Representative photographs of crystal-violet stained cell colonies showed that colony numbers and sizes were increased 769-P/suR than 769-P/suS. The abilities of the 769-P/suR on **(e)** invasion and **(f)** migration were determined using the matrigel invasion assay and scratch test assay, respectively, and the number of cells of 769-P/suR that invaded underside of matrigel membrane and migrated into the wound area were increased compared to the 769-P/suS.

Decreased PD-L1 expression of sunitinib-resistant 769-P cells with transfected siRNA targeting PD-L1

769-P/suR were transfected with siRNA targeting PD-L1 and non-targeting (NCT) siRNA, and the former effectively suppressed the mRNA ($p=0.0001$, Fig. 6A) and protein expression (Fig. 6B) of PD-L1, as measured using quantitative real-time PCR and Western blotting.

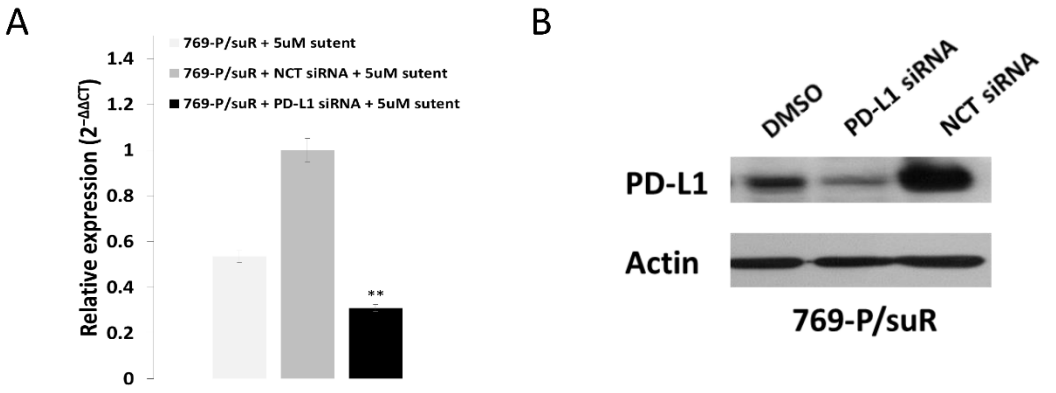

Figure 6 Knockdown of PD-L1 in 769-P/suR. 769-P/suR were transfected with PD-L1 siRNA or NCT, and then subjected to **(a)** qRT-PCR and **(b)** Western blot analysis; GAPDH and Actin were used as loading controls, respectively.

Inhibition of mTOR pathway induces downregulation of PD-L1 in VEGFR-TKI resistance

To evaluate whether PD-L1 expression was dependent on mTOR signaling pathway activation, 769-P/suR was treated with pharmacologic inhibitors -Dactolisib (a dual ATP-competitive PI3K and mTOR inhibitor) and Everolimus (mTOR inhibitor)- of components in the pathway. There was an outstanding decrease in the expression of PD-L1 at the mRNA level (Fig. 7A) in the 769-P/suR treated with Dactolisib (p=0.002) and Everolimus (p=0.028) compared to the 769-P/suS. Both inhibitors decreased PD-L1 expression at the protein level in a time-dependent manner (Fig. 7B). After 72 hours, Inhibition of mTOR signaling pathway appeared to coincide with or precede decreased PD-L1 expression (Fig. 7C).

769-P/suR treated with Dactolisib and Everolimus showed smaller numbers and sizes of colonies compared to 769-P/suR in the colony-forming assay (Fig. 7D). Survival points were 0.09 and 0.63, respectively. Furthermore, not only migration capacity but also invasion capacity was decreased in 769-P/suR treated with Dactolisib and Everolimus in scratch test assay and matrigel invasion assay (Fig. 7E and 7F).

These results suggest that Dactolisib and Everolimus could inhibit the acquired

aggressive behaviors of 769-P/suR and decrease PD-L1 expression by blocking PI3K/Akt/mTOR pathway

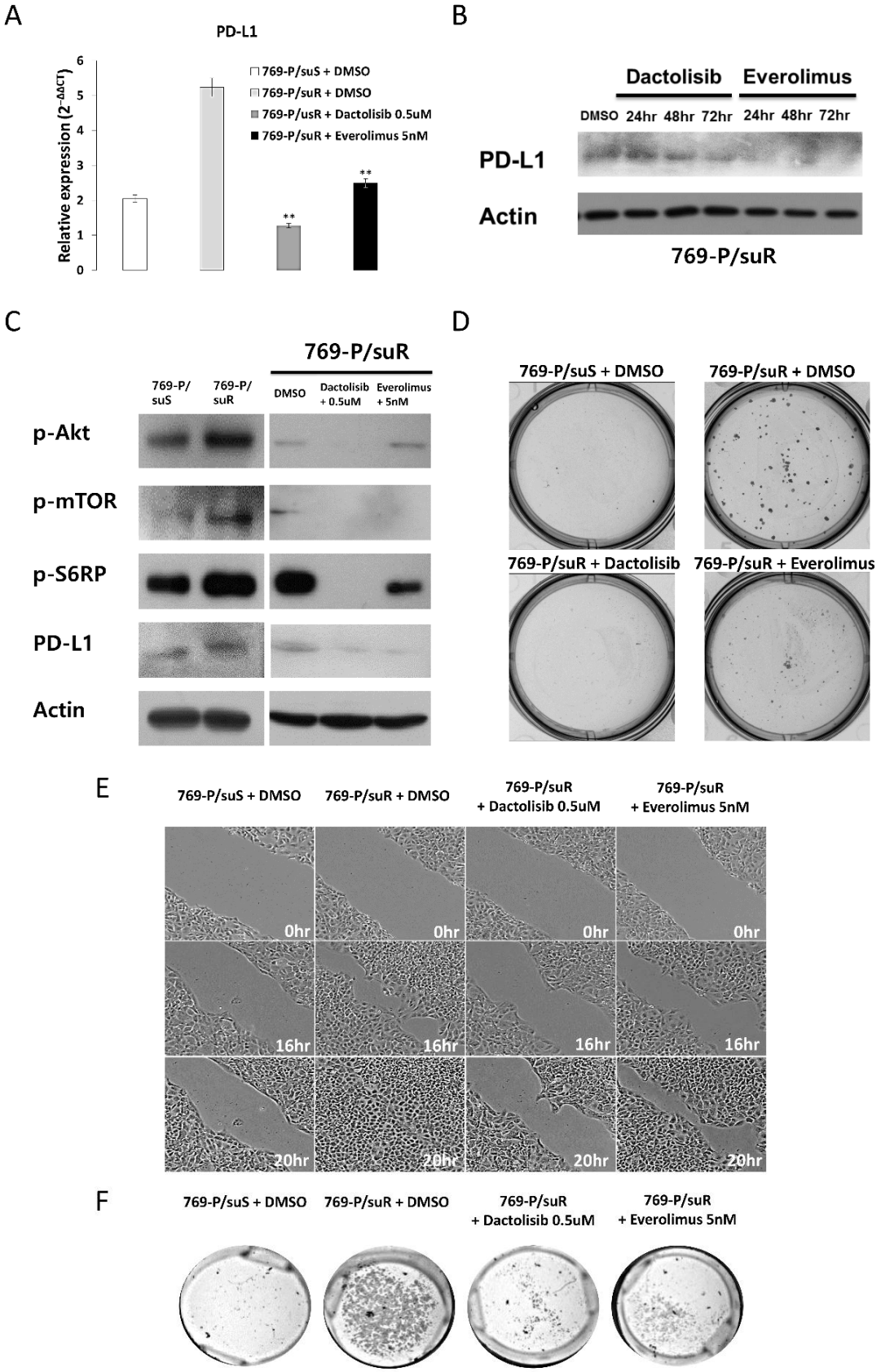
A
PD-L1
Relative expression (2^-ΔΔCT)
769-P/suS + DMSO
769-P/suR + DMSO
769-P/usR + Dactolisib 0.5uM
769-P/suR + Everolimus 5nM
B
Dactolisib
Everolimus
DMSO 24hr 48hr 72hr 24hr 48hr 72hr
PD-L1
Actin
769-P/suR
C
769-P/suR
769-P/ suS
769-P/ suR
DMSO
Dactolisib + 0.5uM
Everolimus + 5nM
p-Akt
p-mTOR
p-S6RP
PD-L1
Actin
D
769-P/suS + DMSO
769-P/suR + DMSO
769-P/suR + Dactolisib
769-P/suR + Everolimus
E
769-P/suS + DMSO
769-P/suR + DMSO
769-P/suR + Dactolisib 0.5uM
769-P/suR + Everolimus 5nM
0hr
16hr
20hr
F
769-P/suS + DMSO
769-P/suR + DMSO
769-P/suR + Dactolisib 0.5uM
769-P/suR + Everolimus 5nM

Figure 7 Down regulated PD-L1 expression and decreased aggressive tumoral behavior in 769-P/suR treated with Dactolisib and Everolimus. **(a)** Down-regulation of PD-L1 expression at the mRNA level in 769-P/suR treated with Dactolisib and Everolimus compared to 769-P/suR + DMSO by qRT-PCR. Data shown in (a) are based on the mean ± SD and p value was obtained using Student's t test. $p < 0.05$ is indicated by "**". **(b)** Inhibition of the mTOR signaling pathway decreases PD-L1 expression of 769-P/suR in a time-dependent manner. **(c)** Dactolisib and Everolimus which inhibits mTOR signaling pathway related proteins reduced PD-L1 expression of 769-P/suR after 72 hours. **(d)** 769-P/suR treated with Dactolisib and Everolimus showed decreased colony numbers and sizes compared to 769-P/suR + DMSO in colony formation assay. **(e)** The ability of the 769-P/suR treated with Dactolisib and Everolimus on migration was determined using the scratch test assay and the number of cells treated with Dactolisib and Everolimus migrated into the wound area were decreased compared to the 769-P/suR + DMSO. **(f)** The ability of the 769-P/suR treated with Dactolisib and Everolimus on invasion was determined using matrigel invasion assay and the number of cells treated with Dactolisib and Everolimus invaded underside of matrigel membrane decreased compared to the 769-P/suR + DMSO.

Discussion

Herein we demonstrated that PD-L1 expression was increased in some patients with, which showed aggressive tumoral behavior compared to TKI-sensitive CCRCC cells in in vitro studies. The mTOR pathway was associated with the PD-L1 upregulation in the VEGFR-TKI resistant CCRCC. In addition, PD-L1 expression is a prognostic indicator for poor PFS in patients with mCCRCC receiving TKI treatment. Therefore, the results revalidated PD-L1/PD-1 and/or mTOR inhibitors may provide therapeutic advantage in VEGFR-TKI resistant CCRCC cases expressing PD-L1.

VEGF has been isolated as an endothelial cell-specific mitogen and mainly functions through binding to VEGF receptors on endothelial cells.[32,33] However, VEGF-mediated autocrine signaling also has been reported in breast carcinoma, squamous carcinoma and glioma to promote the growth, survival, migration, and invasion of tumor cells.[34-38] VEGF-VEGFR signaling pathway of tumor cells was implicated in PI3K/Akt

pathway as dominant signaling pathway in RCC.[39] It activated autophagic mechanism and allowed cancer cells to survive following chemotherapy (docetaxel and Bafilomycin A1) by mTOR complex 1 activity.[40] These reports are in accordance with our results in that endothelium-independent mechanism explains, at least in part, the VEGFR-TKI resistance in CCRCC.

In present study, mTOR pathway was differentially expressed in the pathway analysis of comparing PD-L1-expressing TKI-resistant CCRCC cases to those of PD-L1-non-expressing ones. Furthermore, upregulation of PD-L1 expression by mTOR pathway was verified by *in vitro* and IHC studies. In fact, the upregulation of PD-L1 through the mTOR pathway has been reported in non-small cell lung cancer (NSCLC). In an IHC analysis using human lung cancer where p-S6RP expression was used as a marker of active mTOR signaling, 40% of lung cancer cases had active mTOR signaling and PD-L1 expression with a statistically significant correlation between the two markers (p=0.0001), and a between the two markers where p-S6RP expression were considered positive. Akt/mTOR activation and PD-L1 expression was detected in NSCLC cell lines where not

only PD-L1 expression was decreased by inhibition of PI3K/Akt/mTOR pathway but also induced by EGF and IFN ɣ in an mTOR-dependent manner.[41]

Only a proportion of TKI-resistant CCRCC cases showed PD-L1 expression, 3 cases at the mRNA level and 2 cases at the protein level among 10 those cases in our study. In accordance to our result, clinical studies showed that PD-L1 inhibitor was effective in some of the patients with metastatic CCRCC relapsed after VEGFR-TKI inhibitors. The objective response rates (ORR) of PD-L1 inhibitors (Atezolizumab, Avelumab and Durvalumab) were 12-15%.[42,43] In a clinical study of atezolizumab in advanced RCC, patients with low-to-no expression of PD-L1 (<1%) on tumor and tumor infiltrating immune cell showed trending toward lower antitumor activity compared with patients with PD-L1 expression (≥1%). The ORR for patients with PD-L1 expression was 18% while that of patients with low-to-no PD-L1 expression was 9%. Although there was no obvious difference in the 1-year overall survival rates, 2-year overall survival rates tended to be higher for patients with PD-L1 expression ≥1% versus <1% (65% versus 51%, respectively).[42]

On the other hand, Nivolumab is the first PD-1 inhibitor approved by the FDA on November 2015 for the treatment of patients with advanced RCC.[44] PD-1 inhibitor blocks the interaction between PD-1, expressed on activated T cells, and its ligands including PD-L1, expressed on immune cells and tumor cells, thereby inhibits their cellular immune interactions.[45] In previous studies, the ORR of Nivolumab was 20 to 25% in patients with advanced RCC.[46,47] As shown in present study, they reported that RCC with increased PD-L1 expression was associated with worse prognoses,[5,48,49] although the drug efficacy was observed irrespective of PD-L1 expression.[44] On the other hand, there is an interesting study showing the association of PD-L1 expression and nonresponsiveness of anti PD-1 therapy. Ascierto et al. conducted whole genome microarray and qRT-PCR gene expression analysis using FFPE biopsy tissues from unresectable mRCC patients who received Nivolumab monotherapy. They reported that genes related to metabolic pathway such as glucuronidation were upregulated in non-responder group, while immune markers such as BACH2 and CCL3 overexpressed in responder group.[50] In present study, diverse metabolic pathways such as glycolysis, starch and sucrose metabolism, glucuronidation, and adipogenesis were related to

PD-L1-expressing VEGFR-TKI resistant CCRCC (Tables 4 and 5). Further investigation is required to verify the oncogenic effect of metabolic pathways on VEGF-TKI resistant CCRCC.

This present study had some limitations. There are no impressive difference between the groups expressing PD-L1 and those not. The amount of tissue was insufficient to validate, because some tissues were harvested through needle biopsy. The tissue harvested after VEGFR-TKI resistance development was used in the discovery cohort, but it was not in validation cohort. The validation cohort may be difficult to reflect the whole characteristics of discovery cohort because tissue was harvested before VEGFR-TKI resistance occurs. However, since it is very rare to harvest tissues after VEGFR-TKI resistance has developed, 10 pairs of pre- and post-treatment tumor tissues of discovery cohort are very valuable samples and some cases of them show slightly insufficient but apparent difference in the expression of PD-L1. Present study demonstrated it at the protein and mRNA levels including in vitro study. In the future, further multi-institutional studies to collect paired

samples and more different levels of validation technique including in vivo study are necessary to confirm the results presented here.

References

1. Torre LA, Bray F, Siegel RL, Ferlay J, Lortet Tieulent J, Jemal A. Global cancer statistics, 2012. CA: a cancer journal for clinicians 2015; 65: 87-108.

2. Manola J, Royston P, Elson P*, et al.* Prognostic model for survival in patients with metastatic renal cell carcinoma: results from the international kidney cancer working group. Clinical Cancer Research 2011; 17: 5443-50.

3. Posadas EM, Limvorasak S, Figlin RA. Targeted therapies for renal cell carcinoma. Nat Rev Nephrol 2017; 13: 496-511.

4. Bhat S. Role of surgery in advanced/metastatic renal cell carcinoma. Indian journal of urology: IJU: journal of the Urological Society of India 2010; 26: 167.

5. Thompson RH, Gillett MD, Cheville JC*, et al.* Costimulatory B7-H1 in renal cell carcinoma patients: Indicator of tumor aggressiveness and potential therapeutic target. Proceedings of the National Academy of Sciences of the United States of America 2004; 101: 17174-9.

6. Moch H, Cubilla AL, Humphrey PA, Reuter VE, Ulbright TM. The 2016 WHO classification of tumours of the urinary system and male genital organs—part A: renal, penile, and testicular tumours. European urology 2016; 70: 93-105.

7. Morais C. Sunitinib resistance in renal cell carcinoma. Journal of Kidney Cancer and VHL 2014; 1: 1.

8. Motzer RJ, Rini BI, Bukowski RM*, et al.* Sunitinib in patients with metastatic renal cell carcinoma. Jama 2006; 295: 2516-24.

9. Motzer RJ, Hutson TE, Tomczak P*, et al.* Sunitinib versus interferon alfa in metastatic renal-cell carcinoma. New England Journal of Medicine 2007; 356: 115-24.

10. Escudier B, Eisen T, Stadler WM*, et al.* Sorafenib in advanced clear-cell renal-cell carcinoma. New England Journal of Medicine 2007; 356: 125-34.

11. Mazza C, Escudier B, Albiges L. Nivolumab in renal cell carcinoma: latest evidence and clinical potential. Therapeutic advances in medical oncology 2017; 9: 171-81.

12. Festino L, Botti G, Lorigan P*, et al.* Cancer treatment with anti-PD-1/PD-L1 agents: is PD-L1 expression a biomarker for patient selection? Drugs 2016; 76: 925-45.

13. Black M, Barsoum IB, Truesdell P*, et al.* Activation of the PD-1/PD-L1 immune checkpoint confers tumor cell chemoresistance associated with increased metastasis. Oncotarget 2016; 7: 10557.

14. Hirayama Y, Gi M, Yamano S*, et al.* Anti PD L1 treatment enhances antitumor effect of everolimus in a mouse model of renal cell carcinoma. Cancer science 2016; 107: 1736-44.

15. Brahmer JR, Tykodi SS, Chow LQ*, et al.* Safety and activity of anti–PD-L1 antibody in patients with advanced cancer. N Engl J Med 2012; 2012: 2455-65.

16. Herbst RS, Soria J-C, Kowanetz M*, et al.* Predictive correlates of response to the anti-PD-L1 antibody MPDL3280A in cancer patients. Nature 2014; 515: 563.

17. McDermott DF, Sznol M, Sosman JA*, et al.* Immune correlates and long term follow up of a phase Ia study of MPDL3280A, an engineered PD-L1 antibody, in patients with metastatic renal cell carcinoma (mRCC). Ann Oncol 2014; 25:

18. Hammers H, Plimack E, Infante J*, et al.* Phase i study of nivolumab in combination with ipilimumab (ipi) in metastatic renal cell carcinoma (mrcc). Bju International 2014; 114:

8.

19. Amin A, Plimack ER, Infante JR*, et al.* Nivolumab (anti-PD-1; BMS-936558, ONO-4538) in combination with sunitinib or pazopanib in patients (pts) with metastatic renal cell carcinoma (mRCC): American Society of Clinical Oncology, 2014.

20. Eisenhauer E, Therasse P, Bogaerts J*, et al.* New response evaluation criteria in solid tumours: revised RECIST guideline (version 1.1). European journal of cancer 2009; 45: 228-47.

21. Edge SB, Compton CC. The American Joint Committee on Cancer: the 7th edition of the AJCC cancer staging manual and the future of TNM. Annals of surgical oncology 2010; 17: 1471-4.

22. Eble J. Classification of tumours: pathology and genetics of tumours of the urinary system and male genital organs. World Health Organization Classification of Tumours 2004; 255-7.

23. Smyth GK. Limma: linear models for microarray data. Bioinformatics and computational biology solutions using R and Bioconductor. Springer, 2005; 397-420.

24. Irizarry RA, Wang C, Zhou Y, Speed TP. Gene set enrichment analysis made simple. Stat Methods Med Res 2009; 18: 565-75.

25. Subramanian A, Tamayo P, Mootha VK, *et al.* Gene set enrichment analysis: a knowledge-based approach for interpreting genome-wide expression profiles. Proc Natl Acad Sci U S A 2005; 102: 15545-50.

26. Juengel E, Kim D, Makarević J, *et al.* Molecular analysis of sunitinib resistant renal cell carcinoma cells after sequential treatment with RAD001 (everolimus) or sorafenib. Journal of cellular and molecular medicine 2015; 19: 430-41.

27. Juengel E, Dauselt A, Makarević J, *et al.* Acetylation of histone H3 prevents resistance development caused by chronic mTOR inhibition in renal cell carcinoma cells. Cancer letters 2012; 324: 83-90.

28. Roulin D, Waselle L, Dormond-Meuwly A, Dufour M, Demartines N, Dormond O. Targeting renal cell carcinoma with NVP-BEZ235, a dual PI3K/mTOR inhibitor, in combination with sorafenib. Molecular cancer 2011; 10: 90.

29. Hermann RM, Wolff HA, Jarry H, *et al.* In vitro studies on the modification of low-dose

hyper-radiosensitivity in prostate cancer cells by incubation with genistein and estradiol. Radiation Oncology 2008; 3: 19.

30. Ferrari S, Bandi H, Hofsteenge J, Bussian B, Thomas G. Mitogen-activated 70K S6 kinase. Identification of in vitro 40 S ribosomal S6 phosphorylation sites. Journal of Biological Chemistry 1991; 266: 22770-5.

31. Kumar V, Wollner C, Kurth T, Bukowy JD, Cowley AW. Inhibition of Mammalian Target of Rapamycin Complex 1 Attenuates Salt-Induced Hypertension and Kidney Injury in Dahl Salt-Sensitive RatsNovelty and Significance. Hypertension 2017; 70: 813-21.

32. Leung DW, Cachianes G, Kuang W-J, Goeddel DV, Ferrara N. Vascular endothelial growth factor is a secreted angiogenic mitogen. Science 1989; 246: 1306.

33. Tischer E, Gospodarowicz D, Mitchell R, *et al.* Vascular endothelial growth factor: a new member of the platelet-derived growth factor gene family. Biochemical and biophysical research communications 1989; 165: 1198-206.

34. Barr MP, Bouchier-Hayes DJ, Harmey JJ. Vascular endothelial growth factor is an

autocrine survival factor for breast tumour cells under hypoxia. International journal of oncology 2008; 32: 41-8.

35. Fukasawa M, Matsushita A, Korc M. Neuropilin-1 interacts with integrin β1 and modulates pancreatic cancer cell growth, survival and invasion. Cancer biology & therapy 2007; 6: 1184-91.

36. Bachelder RE, Crago A, Chung J*, et al.* Vascular endothelial growth factor is an autocrine survival factor for neuropilin-expressing breast carcinoma cells. Cancer research 2001; 61: 5736-40.

37. Lichtenberger BM, Tan PK, Niederleithner H, Ferrara N, Petzelbauer P, Sibilia M. Autocrine VEGF signaling synergizes with EGFR in tumor cells to promote epithelial cancer development. Cell 2010; 140: 268-79.

38. Hamerlik P, Lathia JD, Rasmussen R*, et al.* Autocrine VEGF–VEGFR2–Neuropilin-1 signaling promotes glioma stem-like cell viability and tumor growth. Journal of experimental medicine 2012; 209: 507-20.

39. Goel HL, Mercurio AM. VEGF targets the tumour cell. Nature reviews. Cancer 2013;

13: 871.

40. Stanton MJ, Dutta S, Zhang H, *et al.* Autophagy control by the VEGF-C/NRP-2 axis in cancer and its implication for treatment resistance. Cancer research 2013; 73: 160-71.

41. Lastwika KJ, Wilson W, Li QK, *et al.* Control of PD-L1 expression by oncogenic activation of the AKT–mTOR pathway in non–small cell lung cancer. Cancer research 2016; 76: 227-38.

42. McDermott DF, Sosman JA, Sznol M, *et al.* Atezolizumab, an anti–programmed death-ligand 1 antibody, in metastatic renal cell carcinoma: long-term safety, clinical activity, and immune correlates from a phase Ia study. Journal of clinical oncology 2016; 34: 833-42.

43. Weinstock M, McDermott D. Targeting PD-1/PD-L1 in the treatment of metastatic renal cell carcinoma. Therapeutic advances in urology 2015; 7: 365-77.

44. Motzer RJ, Escudier B, McDermott DF, *et al.* Nivolumab versus everolimus in advanced renal-cell carcinoma. New England Journal of Medicine 2015; 373: 1803-13.

45. Medina PJ, Adams VR. PD 1 Pathway Inhibitors: Immuno Oncology Agents for

Restoring Antitumor Immune Responses. Pharmacotherapy: The Journal of Human Pharmacology and Drug Therapy 2016; 36: 317-34.

46. Motzer RJ, Rini BI, McDermott DF, *et al.* Nivolumab for metastatic renal cell carcinoma: results of a randomized phase II trial. Journal of clinical oncology 2014; 33: 1430-7.

47. Atkins M, Clark J, Quinn D. Immune checkpoint inhibitors in advanced renal cell carcinoma: experience to date and future directions. Annals of Oncology 2017; mdx151.

48. Thompson RH, Dong H, Lohse CM, *et al.* PD-1 is expressed by tumor-infiltrating immune cells and is associated with poor outcome for patients with renal cell carcinoma. Clinical cancer research 2007; 13: 1757-61.

49. Thompson RH, Kuntz SM, Leibovich BC, *et al.* Tumor B7-H1 is associated with poor prognosis in renal cell carcinoma patients with long-term follow-up. Cancer research 2006; 66: 3381-5.

50. Ascierto ML, McMiller TL, Berger AE, *et al.* The Intratumoral Balance between

Metabolic and Immunologic Gene Expression Is Associated with Anti–PD-1 Response in Patients with Renal Cell Carcinoma. Cancer immunology research 2016; 4: 726-33.

Abstract

Background: Sunitinib is one of tyrosine kinase inhibitors (TKI) targeting vascular endothelial growth factor (VEGF) - vascular endothelial growth factor receptor (VEGFR) signaling pathways and widely used as a first-line therapy for metastatic clear cell renal cell carcinoma (mCCRCC). However, most patients eventually develop resistance to the drug.

Methods: To define the resistance mechanism regard to upregulation of PD-L1 expression, 10 pairs of TKI-sensitive pre- and TKI-resistant post-treatment mCCRCC tissues were compared for gene expression profile and relating signaling pathway. A separate cohort of 109 cases of mCCRCC treated with VEGFR-TKI was validated by immunohistochemistry and analyzed for progression-free survival (PFS). A sunitinib-resistant renal cancer cell line (769-P/suR) was established after long-term treatment with sunitinib of sensitive 769-P (769-P/suS), then used for in vitro experiments such as MTT assay, qRT-PCR, western blotting, colony-forming assay, scratch test, Matrigel invasion assay, and drug sensitivity test.

Results: PD-L1 expression was increased in post-treatment tissues compared to pre-

treatment tissues in 3 cases among 10 paired CCRCC cases. Pathway analysis showed that the PD-L1 expression was related to the mTOR signaling pathway. These results were validated in separated cohort PD-L1 expression was associated with activation of mTOR pathway in VEGFR-TKI resistant CCRCC and poor PFS in VEGFR-TKI non-responder group. The resistance to sunitinib was confirmed in 769-P/suR, which showed aggressive tumoral behavior such as higher proliferative activity and migration and invasion capacity compared to 769-P/suS. The 769-P/suR showed higher expression of not only PD-L1 but also p-Akt, p-mTOR, and pS6 kinase than 769-P/suS. Blockage of mTOR signaling with mTOR inhibitors in 769-P/suR suppressed PD-L1 expression and reduced the aggressive tumoral behavior.

Conclusions: PD-L1 expression was increased via mTOR pathway at a proportion of VEGFR-TKI resistant CCRCC.